Multiple-Component Scattering Model for Polarimetric SAR Image Decomposition

Lamei Zhang, *Student Member, IEEE*, Bin Zou, *Member, IEEE*,
Hongjun Cai, *Student Member, IEEE*, and Ye Zhang

***Abstract*—A multiple-component scattering model (MCSM) is proposed to decompose polarimetric synthetic aperture radar (PolSAR) images. The MCSM extends a three-component scattering model, which describes single-bounce, double-bounce, volume, helix, and wire scattering as elementary scattering mechanisms in the analysis of PolSAR images. It can be found that double-bounce, helix, and wire scattering are predominant in urban areas. These elementary scattering mechanisms correspond to the asymmetric reflection condition that the copolar and cross-polar correlations are not close to zero. The MCSM is demonstrated with a German Aerospace Center (DLR) Experimental Synthetic Aperture Radar (ESAR) L-band full-polarized image of the Oberpfaffenhofen Test Site Area (DE), Germany, which was obtained on September 30, 2000. The result of this decomposition confirmed that the proposed model is effective for analysis of buildings in urban areas.**

***Index Terms*—Multiple-component scattering model (MCSM), polarimetric synthetic aperture radar (PolSAR), scattering mechanism, target decomposition.**

I. Introduction

POLARIMETRIC synthetic aperture radar (PolSAR) is a well-established technique that allows identification and separation of scattering mechanisms in the polarization signature for purposes of classification and parameter estimation. PolSAR is sensitive to orientation and characters of object, and polarimetry could yield several new descriptive radar target detection parameters and lead to the improvement of radar detection algorithms.

The polarimetric information can reflect the geometric structure and physical characteristic of a target. The polarimetric target decomposition theorem expresses the average mechanism as the sum of independent elements in order to associate a physical mechanism with each resolution cell, which allows the identification and separation of scattering mechanisms in the polarization signature for purposes of classification and recognition. At present, two main classes of decomposition can be identified: 1) coherent decomposition, which deals with decomposition of the scattering matrix, and 2) incoherent decomposition, which deals with coherency or covariance matrices.

Generally, conventional averaging and statistical methods are applied to PolSAR images; therefore, incoherent approaches are frequently chosen for postprocessing. Several decomposition methods have been proposed to identify the scattering characteristics based on polarimetric statistical characteristics [1].

For the natural terrain, Freeman and Durden have proposed a three-component scattering model [2], which decomposes the measured covariance matrix into surface, double-bounce, and volume scattering contributions based on a physical scattering model, as shown in the following:

$$[C]=f_s\begin{bmatrix}|\beta|^2 & 0 & \beta\\ 0 & 0 & 0\\ \beta^* & 0 & 1\end{bmatrix}+f_d\begin{bmatrix}|\alpha|^2 & 0 & \alpha\\ 0 & 0 & 0\\ \alpha^* & 0 & 1\end{bmatrix}+f_v\begin{bmatrix}1 & 0 & 1/3\\ 0 & 2/3 & 0\\ 1/3 & 0 & 1\end{bmatrix} \tag{1}$$

where f_s, f_d, and f_v are the coefficients of the surface, double-bounce, and volume scattering components, respectively.

There are two important assumptions in the Freeman's scattering model. One is that the copolar and cross-polar responses are uncorrelated. The other is that the cross-polar response is generated only by volume scatterers. These assumptions have been validated by experiments in natural areas; therefore, the Freeman's scattering model is a suitable technique to analyze natural distributed areas.

However, in urban areas, the backscattering of an electromagnetic (EM) wave depends on the shape, size, and orientation of the buildings; therefore, the scattering characteristics of urban areas are completely different from those of natural distributed areas. The main difference between natural and urban areas is the correlation coefficient of copolar and cross-polar, i.e., [3]:

$$\langle S_{\mathrm{HH}}S_{\mathrm{HV}}^*\rangle \neq \langle S_{\mathrm{HV}}S_{\mathrm{VV}}^*\rangle \neq 0 \text{ (for urban areas)}$$
$$\langle S_{\mathrm{HH}}S_{\mathrm{HV}}^*\rangle \approx \langle S_{\mathrm{HV}}S_{\mathrm{VV}}^*\rangle \approx 0 \text{ (for natural distributed areas).}$$

Based on the method of Freeman and Durden, Moriyama *et al.* introduced an odd-bounce/even-bounce/cross (OEC) scattering model to represent the polarimetric radar signal from urban areas [3]. Furthermore, Yamaguchi *et al.* extended the three-component decomposition method by adding helix scattering as the fourth component to the three-component scattering model to analyze urban areas [4], [5].

In urban areas, buildings in certain shape, size, and orientation generally exhibit a sharp edge; therefore, wire scattering is supposed as a specific scattering component in urban areas, which is connected with the generation of a cross-polarized response [6].

Manuscript received January 26, 2008; revised May 13, 2008. Current version published October 22, 2008. This work was supported by the National Natural Science Foundation of China under Grant 60672091.

The authors are with the Department of Information Engineering, Harbin Institute of Technology, Harbin 150001, China (e-mail: zzbei@hit.edu.cn).

Color versions of one or more of the figures in this paper are available online at http://ieeexplore.ieee.org.

Digital Object Identifier 10.1109/LGRS.2008.2000795

Considering the properties and structures of buildings, it can be found that double-bounce, helix, and wire scattering are predominant in urban areas [3], [6]. The double-bounce scattering may be caused by dihedral structures of ground and vertical building walls, the helix scattering are relevant for the depolarization of complicated shape of man-made structures, and the wire scattering is formed by edges, eaves, and window frames. These elementary scattering mechanisms correspond to the asymmetric reflection condition that the copolar and cross-polar correlations are not close to zero.

In this letter, we regard single-bounce, double-bounce, volume, helix and wire scattering as the elementary scattering mechanisms in the analysis of PolSAR images. Consequently, a multiple-component scattering model (MCSM) is proposed to decompose PolSAR images.

In Section II, the scattering vector and covariance matrix are briefly summarized. In Section III, we briefly describe the elementary scattering mechanisms in a PolSAR image. Based on these theoretical analyses, we propose an MCSM in Section IV. The experimental results by using L-band Experimental Synthetic Aperture Radar (ESAR) data are derived in Section V. Finally, the conclusion and discussions are presented in Section VI.

II. Scattering Vector and Covariance Matrix

Quad-polarimetric SAR systems measure the 2×2 complex scattering matrix $[S]$ associated with each resolution cell in the image. In the case of backscattering in a reciprocal medium, according to the reciprocity theorem, the 3-D lexicographic scattering vector $\vec{k}_L$ is obtained as

$$\vec{k}_L = \left[S_{\mathrm{HH}}, \sqrt{2}S_{\mathrm{HV}}, S_{\mathrm{VV}}\right]^T. \tag{2}$$

To derive the polarimetric scattering characteristics contained in a PolSAR image, it is necessary to evaluate the second-order statistics of its scattering matrix. The covariance matrix $[C]$ is defined by $\vec{k}_L$, which is shown as

$$[C] = \left\langle \vec{k}_L \vec{k}_L^{*T} \right\rangle = \begin{bmatrix} \langle S_{\mathrm{HH}} S_{\mathrm{HH}}^* \rangle & \langle \sqrt{2} S_{\mathrm{HH}} S_{\mathrm{HV}}^* \rangle & \langle S_{\mathrm{HH}} S_{\mathrm{VV}}^* \rangle \\ \langle \sqrt{2} S_{\mathrm{HV}} S_{\mathrm{HH}}^* \rangle & \langle 2 S_{\mathrm{HV}} S_{\mathrm{HV}}^* \rangle & \langle \sqrt{2} S_{\mathrm{HV}} S_{\mathrm{VV}}^* \rangle \\ \langle S_{\mathrm{VV}} S_{\mathrm{HH}}^* \rangle & \langle \sqrt{2} S_{\mathrm{VV}} S_{\mathrm{HV}}^* \rangle & \langle S_{\mathrm{VV}} S_{\mathrm{VV}}^* \rangle \end{bmatrix} \tag{3}$$

where $\langle \cdot \rangle$ denotes the ensemble average in the data processing, and * denotes the complex conjugation.

The covariance matrix is directly related to the measurable radar parameters and more straightforward to physically understand. Here, we utilize the covariance matrix approach to mathematically derive the MCSM.

III. Elementary Scattering Mechanisms

For the nature and urban areas, there are five elementary scattering mechanisms, i.e., single-bounce, double-bounce, volume, helix, and wire scattering.

A. Single-Bounce Scattering Model

The single-bounce scattering model accounts for the first-order Bragg surface scattering, plate, sphere, and triple-bounce scattering. The scattering matrix for the single-bounce scattering model can be given by

$$[S_s] = \begin{bmatrix} \beta & 0 \\ 0 & 1 \end{bmatrix}, \qquad \mathrm{Re}(\beta) > 0 \tag{4}$$

where β is the ratio of the HH backscatter to the VV backscatter of the single-bounce scattering model. In the first-order Bragg surface case, β is given by

$$\beta = \frac{R_h}{R_v} \qquad \begin{cases} R_h = \frac{\cos\theta - \sqrt{\varepsilon - \sin^2\theta}}{\cos\theta + \sqrt{\varepsilon - \sin^2\theta}} \\ R_v = \frac{(\varepsilon - 1)\left[\sin^2\theta - \varepsilon(1 + \sin^2\theta)\right]}{(\varepsilon\cos\theta + \sqrt{\varepsilon - \sin^2\theta})^2} \end{cases} \tag{5}$$

where θ and ε are the incidence angle and the dielectric constant of the surface, respectively [1]. The covariance matrix for the single-bounce scattering model is

$$[C_s] = \begin{bmatrix} |\beta|^2 & 0 & \beta \\ 0 & 0 & 0 \\ \beta^* & 0 & 1 \end{bmatrix}. \tag{6}$$

B. Double-Bounce Scattering Model

The double-bounce scattering component is modeled by scattering from dihedral structures, including ground and building wall, and ground and trunk.

The scattering matrix for the double-bounce scattering model can be given by

$$[S_d] = \begin{bmatrix} \alpha & 0 \\ 0 & 1 \end{bmatrix}, \qquad \mathrm{Re}(\alpha) < 0 \tag{7}$$

where α is a similar coefficient to β and is defined by

$$\alpha = e^{j2(\gamma_h - \gamma_v)} \frac{R_{\perp h} R_{\parallel h}}{R_{\perp v} R_{\parallel v}} \tag{8}$$

where $R_{\perp h}$ and $R_{\perp v}$ are the horizontal and vertical Fresnel reflection coefficients of the ground surface. Similarly, $R_{\parallel h}$ and $R_{\parallel v}$ are for the vertical wall surface. γ_h and γ_v are the phase attenuation of the horizontal and vertical EM waves, respectively.

The covariance matrix of the double-bounce scattering component is further modeled as

$$[C_d] = \begin{bmatrix} |\alpha|^2 & 0 & \alpha \\ 0 & 0 & 0 \\ \alpha^* & 0 & 1 \end{bmatrix}. \tag{9}$$

C. Volume Scattering Model

For volume scattering, it is assumed that the radar return is from a cloud of randomly oriented very thin dipole scatterers.

The scattering matrix of dipole is shown as

$$[S_{\text{dipole}}] = \begin{cases} \begin{bmatrix} 0 & 0 \\ 0 & 1 \end{bmatrix} & \text{(vertical)} \\ \begin{bmatrix} 1 & 0 \\ 0 & 0 \end{bmatrix} & \text{(horizontal)} \end{cases}. \tag{10}$$

The volume scattering covariance matrix corresponding to the randomly oriented dipoles is simplified as

$$[C_v] = \begin{bmatrix} 1 & 0 & 1/3 \\ 0 & 2/3 & 0 \\ 1/3 & 0 & 1 \end{bmatrix}. \tag{11}$$

D. Helix Scattering Model

Helix scattering is essentially caused by the scattering matrix of helices and is relevant for the complicated shapes of man-made structures, which are predominant in urban areas.

Since the helix target generates circular polarization for all linear polarization incidences, we may regard the term as a source of circular polarization. In fact, for the right helix, we have

$$\begin{aligned}[S_h] &= \frac{1}{2}\begin{bmatrix} 1 & -j \\ -j & -1 \end{bmatrix} \Rightarrow [C_{r-h}] \\ &= \frac{1}{4}\begin{bmatrix} 1 & j\sqrt{2} & -1 \\ -j\sqrt{2} & 2 & j\sqrt{2} \\ -1 & -j\sqrt{2} & 1 \end{bmatrix}\end{aligned} \tag{12}$$

and for the left helix, we have

$$\begin{aligned}[S_h] &= \frac{1}{2}\begin{bmatrix} 1 & j \\ j & -1 \end{bmatrix} \Rightarrow [C_{l-h}] \\ &= \frac{1}{4}\begin{bmatrix} 1 & -j\sqrt{2} & -1 \\ j\sqrt{2} & 2 & -j\sqrt{2} \\ -1 & j\sqrt{2} & 1 \end{bmatrix}.\end{aligned} \tag{13}$$

E. Wire Scattering Model

The backscattering response from urban areas can be decomposed into copolar and cross-polar components. In urban areas, the dihedral structures formed by ground and vertical building walls and the wire scattering derived by the edges in the buildings are connected with the generation of a cross-polarized response.

Wire scattering is a specific scattering component in urban areas. The characteristic scattering matrix of the canonical thin-wire target has been described in [3] and [6] as a function of the orientation angle around the line of sight. A general wire scattering model, which represents the remaining component of urban areas, can be expressed as the following scattering matrix:

$$[S_w] = \begin{bmatrix} \gamma & \rho \\ \rho & 1 \end{bmatrix} \tag{14}$$

where γ and ρ are the ratios of the HH and HV backscatters to the VV backscatter, respectively, i.e.,

$$\gamma = \frac{S_{\text{HH}}}{S_{\text{VV}}} \qquad \rho = \frac{S_{\text{HV}}}{S_{\text{VV}}}. \tag{15}$$

The corresponding covariance matrix is obtained as

$$[C_w] = \begin{bmatrix} |\gamma|^2 & \sqrt{2}\gamma\rho^* & \gamma \\ \sqrt{2}\gamma^*\rho & 2|\rho|^2 & \sqrt{2}\rho \\ \gamma^* & \sqrt{2}\rho^* & 1 \end{bmatrix}. \tag{16}$$

IV. MCSM

Based on the analysis of the aforementioned elementary scattering models, the MCSM is proposed, describing single-bounce, double-bounce, volume, helix, and wire scattering as elementary scattering mechanisms in the analysis of PolSAR images. Therefore, the covariance matrix can be expressed as

$$[C] = f_s[C_s] + f_d[C_d] + f_v[C_v] + f_h[C_h] + f_w[C_w] \tag{17}$$

where f_s, f_d, f_v, f_h, and f_w are the coefficients to be determined. Comparing the covariance matrix elements, we obtain the following six equations:

$$\left\langle |S_{\text{HH}}|^2 \right\rangle = f_s|\beta|^2 + f_d|\alpha|^2 + f_v + \frac{1}{4}f_h + f_w|\gamma|^2 \tag{18a}$$

$$\left\langle |S_{\text{VV}}|^2 \right\rangle = f_s + f_d + f_v + \frac{1}{4}f_h + f_w \tag{18b}$$

$$\langle S_{\text{HH}}S_{\text{VV}}^* \rangle = f_s\beta + f_d\alpha + \frac{1}{3}f_v - \frac{1}{4}f_h + f_w\gamma \tag{18c}$$

$$\left\langle |S_{\text{HV}}|^2 \right\rangle = \frac{1}{3}f_v + \frac{1}{4}f_h + f_w|\rho|^2 \tag{18d}$$

$$\langle S_{\text{HH}}S_{\text{HV}}^* \rangle = \pm j\frac{1}{4}f_h + f_w\gamma\rho^* \tag{18e}$$

$$\langle S_{\text{HV}}S_{\text{VV}}^* \rangle = \pm j\frac{1}{4}f_h + f_w\rho. \tag{18f}$$

The wire scattering coefficient f_w and the helix scattering coefficient f_h can be obtained from (18e) and (18f), as shown in the following:

$$f_w = \frac{\langle S_{\text{HH}}S_{\text{HV}}^* \rangle - \langle S_{\text{HV}}S_{\text{VV}}^* \rangle}{\gamma\rho^* - \rho} \tag{19}$$

$$f_h = 2\text{Im}\left\{\langle S_{\text{HH}}S_{\text{HV}}^* \rangle + \langle S_{\text{HV}}S_{\text{VV}}^* \rangle - f_w(\gamma\rho^* + \rho)\right\}. \tag{20}$$

Then, (18d) directly gives the volume scattering coefficient f_v, as shown in the following:

$$f_v = 3\left\{\left\langle |S_{\text{HV}}|^2 \right\rangle - \frac{1}{4}f_h - f_w|\rho|^2\right\}. \tag{21}$$

The remaining unknowns can be obtained in the same manner as shown in [2]. Therefore, the scattering powers P_s, P_d, P_v, P_h, and P_w, which correspond to the single-bounce,

(a)

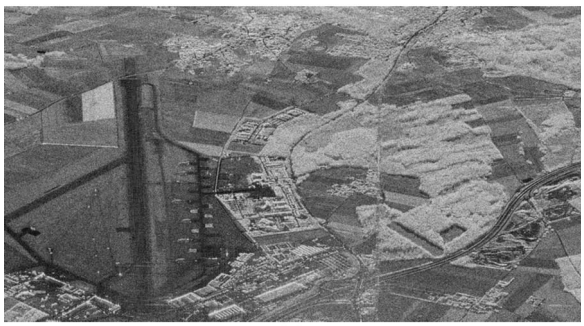

(b)

Fig. 1. Test data of ESAR. (a) Optical image. (b) HH channel image.

double-bounce, volume, helix, and wire scattering contributions, respectively, are estimated as

$$\begin{aligned} P_s &= f_s\left(1+|\beta|^2\right) \\ P_d &= f_d\left(1+|\alpha|^2\right) \\ P_v &= 8f_v/3 \\ P_h &= f_h \\ P_w &= f_w\left(1+|\gamma|^2+2|\rho|^2\right) \\ P &= P_s+P_d+P_v+P_h+P_w. \end{aligned} \tag{22}$$

Equations (17)–(22) are the main set of expressions for the MCSM. Compared with the three-component scattering model, the helix and wire scattering mechanisms, which correspond to the copolar and cross-polar correlations, are introduced for a more general target decomposition method. The helix and wire scattering often appear in complex urban areas, but they disappear in almost all natural distributed scenarios.

V. Experimental Results and Discussion

A German Aerospace Center (DLR) ESAR L-band full-polarized data set of the Oberpfaffenhofen Test Site Area (DE), Germany, which was obtained on September 30, 2000, was used to validate the proposed decomposition method. The spatial resolution of the test data is 3 m × 3 m. The optical and HH channel images are shown in Fig. 1(a) and (b), respectively. The test area is mainly composed of forest, several kinds of farmland, runway, and man-made buildings. A color image of the classical Pauli decomposition is shown in Fig. 2, with α (red), β (green), and γ (blue).

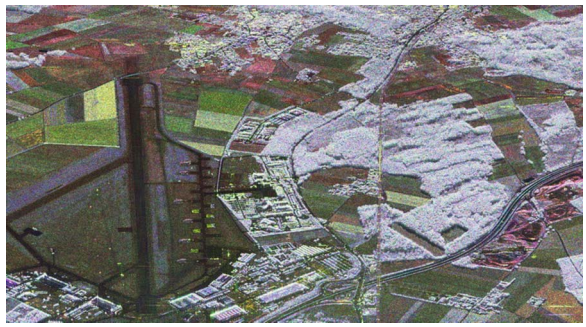

Fig. 2. Pauli decomposition. The image is colored red (α), green (β), and blue (γ).

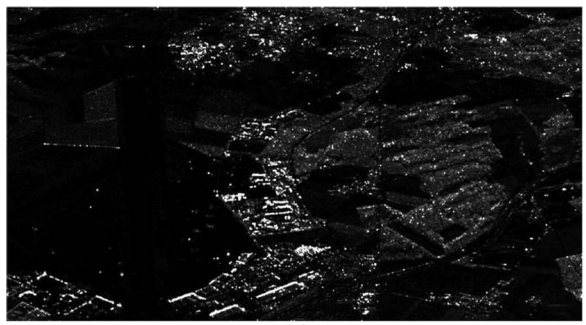

(a)

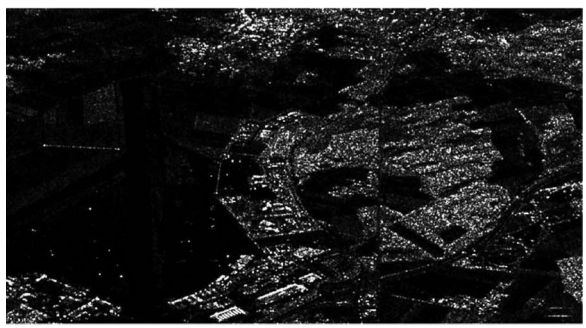

(b)

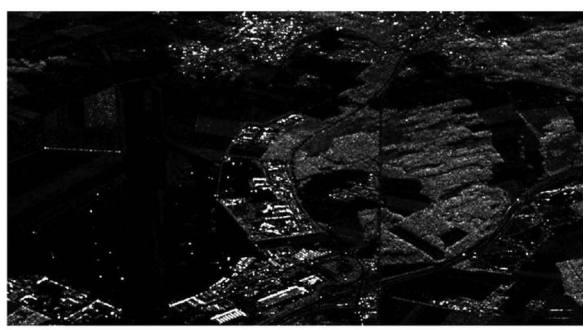

(c)

Fig. 3. Result of the MCSM. (a) Power image of P_d. (b) Power image of P_h. (c) Power image of P_w.

As previously discussed in this letter, in urban areas, building blocks produce a rather predominant HV response. Therefore, the helix and wire scattering components appear stronger in these areas. Fig. 3(a)–(c) shows the scattering powers of double-bounce, helix, and wire scattering, respectively. Comparing Fig. 3 with Fig. 1(a), we found that the double-bounce, helix, and wire scattering components in urban areas are

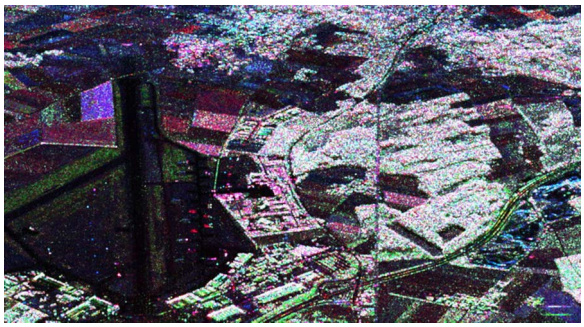

Fig. 4. MCSM decomposition. The image is colored red (P_d), green (P_v), and blue (P_s).

stronger than those of the farmland and forest areas. Double-bounce and wire scattering are prominent for buildings, particularly at the edge of buildings parallel to the SAR flight path.

Fig. 4 shows the decomposition result of the MCSM, which is colored red (P_d), green (P_v), and blue (P_s). The buildings in the middle and at the left bottom have stronger scattering powers compared with those in Fig. 1(b), particularly at the edge of buildings. The blue area in the upper left and lower right corresponds to farmland, which shows that surface scattering is prominent. The upper forest area is decomposed to be a green area, indicating that volume scattering is prominent. The pink-colored area in the middle is a large area of forest, where double-bounce and surface scattering are equally strong due to arborous foliage.

A typical feature of urban areas containing geometrically complicated man-made buildings is that $\langle|S_{\rm HV}|^2\rangle$ is rather predominant compared with $\langle|S_{\rm HH}|^2\rangle$ and $\langle|S_{\rm VV}|^2\rangle$. As previously discussed, the MCSM is suitable for characterization of man-made buildings in urban areas containing helix and wire scattering components, corresponding to the cross-polarized response. On the other hand, the Freeman's three-component model has been validated in the forest area [2].

The theoretical studies show that copolar and cross-polar channel powers are statistically of a magnitude ratio of $2:1$. Consequently, the MCSM and Freeman's method are chosen based on the following ratio: $2\langle|S_{\rm HV}|^2\rangle : \langle|S_{\rm HH}|^2\rangle$ or $\langle|S_{\rm VV}|^2\rangle$.

VI. Conclusion

An MCSM based on the covariance matrix is proposed for polarimetric SAR decomposition, which is intended to be applied to the general conditions, including both the nonreflection symmetry case and the reflection symmetry condition. The MCSM is an extension of the three-component decomposition. In the MCSM, single-bounce, double-bounce, volume, helix, and wire scattering are regarded as elementary scattering mechanisms in the analysis of PolSAR images. Compared with the Freeman's method, the helix and wire scattering components related with the cross-polarized response are added for a more general scattering mechanism, which are relevant for the complicated shapes of man-made structures in urban areas. The MCSM should be able to theoretically analyze a general condition. In this letter, we focus on the urban area application. These preliminary results with the implementation of L-band ESAR PolSAR data show that the proposed model is effective for analysis of urban areas. In the future, more experiments using different data of different fields will be done, and the interpretation of the decomposition results and the performance of the MCSM will be studied.

References

[1] S. R Cloude and E. Pottier, "A review of target decomposition theorems in radar polarimetry," *IEEE Trans. Geosci. Remote Sens.*, vol. 34, no. 2, pp. 498–518, Mar. 1996.

[2] A. Freeman and S. L. Durden, "A three-component scattering model for polarimetric SAR data," *IEEE Trans. Geosci. Remote Sens.*, vol. 36, no. 3, pp. 963–973, May 1998.

[3] T. Moriyama, S. Uratsuka, T. Umehara *et al.*, "Polarimetric SAR image analysis using model fit for urban structures," *IEICE Trans. Commun.*, vol. E88-B, no. 3, pp. 1234–1242, Mar. 2005.

[4] Y. Yamaguchi and T. Moriyama, "Four-component scattering model for polarimetric SAR image decomposition," *IEEE Trans. Geosci. Remote Sens.*, vol. 43, no. 8, pp. 1699–1706, Aug. 2005.

[5] Y. Yamaguchi, Y. Yajima, and H. Yamada, "A four-component decomposition of PolSAR images based on the coherency matrix," *IEEE Geosci. Remote Sens. Lett.*, vol. 3, no. 3, pp. 292–296, Jul. 2006.

[6] E. Krogager, W. M. Borner, and S. N. Madsen, "Feature-motivated Sinclair matrix (sphere/diplane/helix) decomposition and its application to target sorting for land feature classification," *Proc. SPIE*, vol. 3120, pp. 144–154, Jul. 28–29, 1997.